NATIONAL ADVISORY COMMITTEE
FOR AERONAUTICS

TECHNICAL NOTE 3850

EXPERIMENTAL INVESTIGATION ON THE LANGLEY HELICOPTER TEST

TOWER OF COMPRESSIBILITY EFFECTS ON A ROTOR

HAVING NACA 63_2-015 AIRFOIL SECTIONS

By James P. Shivers and Paul J. Carpenter

Langley Aeronautical Laboratory
Langley Field, Va.

Washington
December 1956

NATIONAL ADVISORY COMMITTEE FOR AERONAUTICS

TECHNICAL NOTE 3850

EXPERIMENTAL INVESTIGATION ON THE LANGLEY HELICOPTER TEST

TOWER OF COMPRESSIBILITY EFFECTS ON A ROTOR

HAVING NACA 63_2-015 AIRFOIL SECTIONS

By James P. Shivers and Paul J. Carpenter

SUMMARY

An investigation has been conducted on the Langley helicopter test tower to determine experimentally the effects of compressibility on the hovering performance and the blade pitching moments of a helicopter rotor having NACA 63_2-015 airfoil sections. Data are presented for blade tip Mach numbers from 0.31 to 0.71.

The results show that the rotor having NACA 63_2-015 airfoil sections can operate at much higher mean blade lift coefficients before encountering compressibility losses than were indicated from previous tests of rotors having NACA 23015 airfoil sections. At a tip Mach number of 0.71, mean blade lift coefficients of about 0.6 were reached without any appreciable compressibility losses.

The results show that the two-dimensional airfoil-section data provide a reasonable basis for predicting the onset of compressibility losses and that the differences in Mach number for drag divergence between airfoils shown by two-dimensional data are realized in actual rotor tests.

INTRODUCTION

One method of meeting the requirements of increased helicopter speeds and higher disk loadings is by increasing the rotor-blade tip Mach number. Design studies of helicopters with rotor tip speeds in the high subsonic Mach number range and with high blade loadings have emphasized the need for experimental rotor performance and blade pitching-moment data on rotors operating in the region of compressibility effects.

Some initial data on the effects of compressibility on rotor hovering performance have been obtained with rotor blades having NACA 23015 airfoil sections (ref. 1). The objective of that investigation was the

determination of the effects of compressibility for that rotor and the
extent to which the compressibility drag rise could be predicted from
available two-dimensional-airfoil-section data.

The present investigation, which is an extension of that of ref-
erence 1, was conducted with a rotor having NACA 63_2-015 airfoil sections.
The purpose of this investigation was to determine the effects of com-
pressibility on rotor performance and the extent to which the onset of
compressibility drag rise could be predicted for a rotor blade having
the same thickness ratio as that of reference 1 but with a chordwise
thickness distribution more favorable for high-tip-speed performance.
Inasmuch as no high-speed two-dimensional section drag data for the NACA
63_2-015 airfoil were available, unpublished two-dimensional section data
for the NACA 64_2-015 airfoil were used to make a comparison with the
experimental rotor drag divergence. (These data remain unpublished since
they include an undetermined tare in the section drag coefficient and
the maximum lift coefficients are uncertain.) This particular rotor was
selected for study because the NACA 63_2-015 airfoil is one of those con-
sidered for low-pressure pressure-jet application wherein the rotor
blades must meet the dual requirements of operating at high tip speeds
and yet have large internal volume for air ducts. Also, compressibility
losses can be studied at lower tip speeds than for thinner sections; thus,
some of the structural problems encountered in tests at high tip speeds
are alleviated.

The rotor blades were tested on the Langley helicopter test tower
over a tip Mach number range from 0.31 to 0.71 (disk loading up to 7 pounds
per square foot) with a corresponding blade tip Reynolds number range
from 2.19×10^6 to 4.96×10^6. Inasmuch as the rotor-blade leading edge
may become rough in field service due to abrasions or to the accumula-
tion of foreign particles, such as bug spatters, the tests were repeated
for three tip Mach numbers (0.46, 0.62, and 0.71) with NACA standard
leading-edge roughness.

Drag and lift curves as a function of blade angle of attack and
Mach number were synthesized by using the rotor experimental data and
unpublished data on the NACA 64_2-015 airfoil. Such information should
be useful in predicting the onset of compressibility power losses and
their rate of growth for rotors having similar airfoils.

SYMBOLS

a   slope of section-lift-coefficient curve as a function of section
           angle of attack (radian measure), assumed to be 5.73

b   number of blades per rotor

C_M measured blade pitching-moment coefficient, $\dfrac{M}{1/2\rho c^2(\Omega R)^2 R}$

C_Q rotor torque coefficient, $\dfrac{Q}{\pi R^2 \rho (\Omega R)^2 R}$

$C_{Q,o}$ rotor profile-drag torque coefficient, $\dfrac{Q_o}{\pi R^2 \rho (\Omega R)^2 R}$

C_T thrust coefficient, $\dfrac{T}{\pi R^2 \rho (\Omega R)^2}$

c blade section chord at radius r, ft

c_d blade drag coefficient

$c_{d,o}$ section profile-drag coefficient

c_l airfoil section lift coefficient

$\overline{c_l}$ mean rotor-blade lift coefficient, $\dfrac{6C_T}{\sigma}$

M measured pitching moment of a rotor blade, lb-ft

M_t tip Mach number

N_{Re} Reynolds number, $\dfrac{\rho \Omega R c}{\mu}$

Q total rotor torque, lb-ft

Q_o rotor profile-drag torque, lb-ft

R blade radius, ft

r radial distance to a blade element, ft

T rotor thrust, lb

x ratio of blade element radius to full radius, r/R

α angle of attack, deg

α_r blade section angle of attack, deg

θ blade-section pitch angle measured from line of zero lift, radians

μ coefficient of viscosity, slugs/ft-sec

ρ mass density of air, slugs/cu ft

σ rotor solidity, $bc/\pi R$, 0.0374

σ_x rotor solidity at spanwise station x

φ inflow angle at blade element, $\dfrac{\sigma_x a}{16x}\left(\sqrt{1 + \dfrac{32x\theta}{\sigma_x a}} - 1\right)$, radians

Ω rotor angular velocity, radian/sec

Subscript:

t rotor tip

APPARATUS AND TEST METHODS

The investigation reported herein was conducted on the modified version of the Langley helicopter test tower described in reference 2. Modification consisted of enlarging the working area at the base of the tower and repowering with a 3,000-horsepower variable-frequency electric drive motor. The rotor, as tested, was a fully articulated two-blade rotor with the flapping hinge located on the center line of rotation and the drag hinge 12 inches outboard of the center line. A photograph of the rotor installation on the Langley helicopter test tower is presented in figure 1.

Rotor Blades

The rotor blades used in the investigation were of all-metal construction and had NACA 63_2-015 airfoil sections. The rotor blades were of rectangular plan form with a chord of 13 inches, a radius of 18.41 feet, a solidity of 0.0374, and had 6.5° of linear negative twist between the center of rotation and the blade tip. A single rotor blade as tested weighed 60 pounds and had a spanwise center of gravity at 48.2 percent of

the radius and a chordwise center of gravity at 26.8 percent chord from the leading edge. The pitch axis of the rotor blade was located at 10.3 percent chord from the leading edge.

The main spar was a tubular-steel D-section located at the leading edge of the airfoil. The outside of the airfoil was formed by a single wrapping of stainless-steel skin cemented together at the trailing edge. The rearward 75 percent of the airfoil skin was reinforced with chordwise hat sections bonded internally to the stainless-steel skin and to the main spar.

The rotor blade was a factory production model and deviated slightly from a true NACA 63_2-015 airfoil section; however, the airfoil was smooth and free from flat spots over most of the blade span in the area extending back to about 20 percent of its chord. A convenient indication of relative smoothness of the rotor-blade surfaces is given by the zero-lift profile-drag coefficient. The present production blade of which the skin surface is hereinafter referred to as "smooth" had a zero-lift drag coefficient of 0.0086. With standard NACA leading-edge roughness, the drag coefficient at zero lift increased to about 0.012. If the blade had had an aerodynamically smooth surface, the drag coefficient would be expected to be about 0.005.

Tests were also made with leading-edge roughness added to the forward 8 percent of the blade chord over the entire blade span. The leading-edge roughness was standard NACA leading-edge roughness used in wind-tunnel airfoil tests (ref. 3). The roughness consisted of 0.011-inch-diameter carborundum particles applied over a surface length corresponding to 8 percent of the chord back from the leading edge on the upper and lower surfaces. The particles covered from 5 to 10 percent of this area.

A resistance-type strain gage, mounted on the rotor-blade main spar at about the 20-percent-radius station, was used to monitor the blade stresses so that the test conditions would not exceed the estimated yield stress of the blade-spar material.

Test Methods and Accuracy

The test procedure was to set a given tip Mach number and then vary the blade pitch through a range from zero thrust to the point where an increase in blade pitch did not increase rotor thrust, except in the high-tip-speed range where the blade stresses limited the allowable pitch range. At each pitch setting, data were recorded both from visual dial readings and on an oscillograph. Quantities measured were rotor thrust, rotor torque, blade pitch angle, blade pitching moment, rotor shaft rotational speed, blade drag angle, and blade flapping angle. The range of

test conditions was chosen to exceed the tip Mach number corresponding
to the force break in order to establish the rate of increase of compressibility losses with tip angle of attack and Mach number.

The estimated accuracies of the basic quantities measured during
the tests are as follows: rotor thrust, ±20 pounds; rotor torque,
±50 foot-pounds; rotor rotational speed, ±1 revolution per minute; and
all angular measurements, ±0.2°. The overall accuracy of the plotted
results is believed to be within ±3 percent.

METHOD OF ANALYSIS

In order to show the onset and rate of growth of the compressibility
drag rise and drag increase due to blade stall past the blade section
maximum lift, that part of the power affected by these losses had to be
isolated. An analysis of the problem indicates that the profile-drag
power and, hence, the profile-drag torque coefficient would be chiefly
affected.

A convenient method of showing the rate of growth of profile torque
losses for the range of tip Mach numbers investigated is to use a ratio
of profile-drag torque coefficient deduced from the test results to that
calculated by using conventional strip analysis and to plot the resulting

ratios $\frac{C_{Q,o}(\text{measured})}{C_{Q,o}(\text{calculated})}$ as a function of the blade-tip angle of attack.

The assumption used in obtaining the calculated $C_{Q,o}$ at a given rotor
C_T was the conventional airfoil drag polar

$$c_{d,o} = 0.0087 - 0.0216\alpha_r + 0.400\alpha_r^2$$

and a linear lift-coefficient slope

$$c_l = a\alpha_r$$

This drag polar has been used in several analyses (refs. 4 to 7)
and experience has shown that it is a good approximation of the low-
speed profile drag of well-built, semismooth blades below the section
maximum lift. The measured rotor profile-drag torque coefficients were
determined by subtracting a calculated induced torque coefficient from
the measured torque coefficient.

The data were plotted as a function of tip angle of attack inasmuch
as the tip-section angle of attack and tip Mach number are an index of
the compressibility losses.

The rotor-blade-tip angles of attack were determined by first plotting the rotor thrust coefficient as a function of measured rotor-tip pitch angle. Secondly, a calculated tip inflow angle φ_t was obtained from strip analysis and was plotted as a function of calculated rotor thrust coefficient. At a given experimental rotor thrust coefficient, the tip angle of attack was obtained by subtracting the calculated inflow angle φ_t obtained at the same thrust coefficient from the measured tip pitch angle θ.

The measured blade pitching moments consisted of moments due to aerodynamic and mass forces and, since they were small, no attempt has been made to separate them into individual components. The measured moments have been reduced to nondimensional coefficients.

The blade pitching moments were obtained by measuring the forces in the blade pitch controls. At zero lift, the moments are those about the pitch axis which is located 10.3 percent from the chord leading edge. As the lift is increased, another moment appears which is a moment about the blade center of gravity and is equal to the product of the blade lift and the distance between the center of gravity and the aerodynamic center. There also exists a moment due to centrifugal forces which acts to restore the blade section to flat pitch, but it is small and has been ignored.

No attempts were made to obtain the blade aerodynamic moment by subtracting the moment due to the displacement of the center of gravity from the aerodynamic center. Inasmuch as the aerodynamic-center position, especially with respect to high tip speeds, is not precisely known and the position of the aerodynamic center with respect to the blade center of gravity has a very powerful effect on the blade pitching moment, no correction to the data has been made. Thus, more significance should be attached to the presence or absence of abrupt changes of pitching-moment slopes rather than to the actual values.

RESULTS AND DISCUSSION

The basic hovering performance and rotor blade pitching-moment curves are presented first. From these basic curves, a detailed analysis of the effects of compressibility and stall are presented, together with a comparison of the test rotor blades with the rotor of reference 1. Synthesized rotor-blade airfoil data that can be used to predict high-tip-speed performance of rotors having similar airfoil sections are also shown.

Hovering Performance

Smooth blades.- The hovering performance of the smooth blades is shown in figure 2 as plots of thrust coefficient as a function of torque coefficient for blade-tip Mach numbers of 0.31 to 0.71. A calculated rotor-performance curve based on a linear lift=coefficient slope

$$c_l = a\alpha_r$$

and conventional drag polar

$$c_{d,o} = 0.0087 - 0.0216\alpha_r + 0.400\alpha_r^2$$

is also plotted for comparison with the experimental data. The calculated curve was obtained by using conventional strip-analysis procedure and a 3-percent-tip loss factor (outer 3 percent of the blade produces no lift but has profile drag). In general, the experimental low-tip-speed curves show excellent agreement with the calculated curve up to a thrust coefficient of about 0.0050 to 0.0060 $\left(\overline{c_l} = 0.804\right)$.

Increases in tip speed caused the experimental rotor-performance curve to break away from the calculated curve at progressively lower values of thrust-coefficient. The breakaway point of the experimental curve from the calculated curve indicates the critical value at which compressibility and stall losses begin.

It is significant that, although this rotor blade had a 15-percent-thick airfoil section, a rotor thrust coefficient of about 0.0037 $\left(\overline{c_l} = 0.6\right)$ was obtained at a tip Mach number of 0.71 with only about a 4.4-percent increase in power due to compressibility losses.

Leading-edge roughness.- Since helicopter rotor blades may develop leading-edge roughness during normal service because of abrasion or the accumulation of foreign particles, a portion of the test program was repeated with standard NACA leading-edge roughness applied to the rotor blades. This roughness probably represents more than that usually due to normal service and is used only to demonstrate the effects of an extreme condition.

A comparison of the rotor performance with smooth blades $\left(M_t = 0.46, 0.62, \text{ and } 0.71\right)$ and with leading-edge roughness $\left(M_t = 0.44, 0.62, \text{ and } 0.72\right)$ applied is shown in figure 3. The addition of leading-edge roughness increased the zero-thrust profile-torque coefficient by about 40 percent. The increment in profile torque increases as thrust coefficient is increased and at a tip Mach number of 0.46 and a thrust coefficient of 0.0050, the increment increase in profile torque due to roughness is about 3.5 times that shown at zero thrust. The leading-edge roughness reduced the maximum rotor thrust coefficient and at the highest tip Mach number reduced the rotor thrust coefficients at which the compressibility

drag rise started to occur. For example, at a tip Mach number of 0.71, the rotor thrust coefficient for compressibility drag rise is about 0.001 less than that shown for the smooth blades.

Rotor Blade Pitching Moments

Rotor-blade pitching-moment data are necessary to determine the rotor control forces and are important in blade vibration and stability analyses.

Smooth blades.- A comparison of the blade pitching-moment character- istics for tip Mach numbers of 0.31 to 0.71 for the rotor tested in the smooth condition as a function of rotor thrust coefficient is shown in figure 4. The pitching-moment data represent the measured rotor blade moments about the blade pitch axis and include both aerodynamic and blade mass forces.

The moments shown at zero rotor thrust coefficient are presumably due to deviations of the airfoil from a truly symmetrical section. The change in blade moments as thrust is increased may be partly due to devi- ation from true airfoil contour but probably is largely caused by the displacement of the blade aerodynamic center from the blade center of gravity. As mentioned previously, the blade aerodynamic center is not precisely known. Since the position of the aerodynamic center with respect to the center of gravity has a very powerful effect on blade pitching moments and since the actual measured moments are small (-10 ft-lb to 90 ft-lb), it appears more logical to present the total measured moments about the pitch axis of the blade.

At the lower tip Mach numbers (below $M_t = 0.46$), the pitching moments are negative (that is, nose down) throughout the thrust-coefficient range. At the higher thrust coefficient, the pitching-moment curve slope reverses; this reversal indicates a rearward shift in center of pressure due to blade stall. The effect of increasing the tip Mach number was to shift the center of pressure forward slightly and thus produce nose-up moments and to decrease the thrust coefficient at which the pitching-moment curve slope reverses.

The point at which compressibility or stall begins to increase the rotor power requirement is noted by a tick on the curves (fig. 4). It is significant that, although the tip of the blade is encountering com- pressibility losses, the reversal in slope of the blade pitching-moment curve is delayed well beyond the onset of compressibility losses. This characteristic is also shown by the unpublished data on the two- dimensional NACA 64_2-015 airfoil section. At the higher tip Mach num- bers, rotor data were not obtained at a high enough thrust coefficient to determine the pitching-moment reversal. (Allowable blade bending

stresses limited the data obtainable.) In general, more significance
should be attached to the shape of these curves than to their actual
numerical values.

Leading-edge roughness.- The effect of leading-edge roughness on
the blade pitching moments is shown in figure 5 for tip Mach numbers
of 0.44, 0.62, and 0.72. Leading-edge roughness shifts the pitching-
moment curves to a positive or nose-up moment over most of the thrust-
coefficient range. This shifting indicates that the center of pressure
is slightly forward as compared with the smooth condition. The thrust-
coefficient value at which the pitching-moment curve slope reverses is
also substantially less (15 to 25 percent) than that obtained for the
blade in the smooth condition.

The point at which compressibility begins to increase the rotor
power requirements is noted by a tick on the curves of figure 5. It is
significant here also that, although the tip of the blade is encountering
compressibility losses, the reversal in slope of the blade pitching-
moment curve is delayed beyond the onset of compressibility losses.

In general, the overall effects of leading-edge roughness are an
increase in profile drag, a decrease in maximum rotor thrust coefficient,
a decrease in rotor thrust coefficient for compressibility drag rise
and for the break in the pitching-moment curves.

Rotor Profile Drag Torque

The principal effect of compressibility and stall on the rotor is
an increase in the rotor profile drag torque. The dividing line between
stalling losses and compressibility losses is never clearly defined and
these losses are usually combined. In general, however, stalling losses
are predominant in the lower subsonic blade-tip Mach number range at high
angles of attack and compressibility losses are predominant at the higher
blade-tip subsonic Mach numbers and lower angles of attack.

Figure 6 presents the ratios of $C_{Q,o(measured)}$ to $C_{Q,o(calculated)}$,
based on the aforementioned assumption of linear lift-curve slope and con-
ventional drag polar, plotted as a function of calculated blade-tip angle
of attack. At the lower tip Mach numbers ($M = 0.31$ to $M = 0.40$), the
ratio of profile-drag torque coefficients remains near unity up to cal-
culated blade-tip angles of about 10°; this condition indicates that
there was no drag increase over and above that represented by the con-
ventional drag polar. Above blade tip angles of 10°, the profile-drag
torque coefficient ratios begin to diverge from unity; this divergence
indicates an increased drag due to flow separation on the airfoil. At
the lowest tip Mach number of 0.31, the drag increase occurred at a
lower tip angle (about 9.4°) than at the next highest tip Mach number

of 0.36. This condition is probably due to the beneficial effect of a higher Reynolds number in delaying separation. The effect of a reduction on maximum section lift coefficient with a reduction in Reynolds number, in the test region previously discussed, has also been shown in the two-dimensional data of reference 8.

At the lower blade-tip Mach numbers as the tip angle is increased about 2° past the onset of blade stall, the profile torque losses are about 40 percent greater than that calculated by using the conventional drag polar. At the higher blade-tip Mach number, the initial rate of growth of the compressibility losses indicates about a 50-percent increase in profile-drag torque losses for 2° of blade-tip angle increase past the onset of compressibility losses.

Comparison With Two-Dimensional Drag-Divergence Data

Since the compressibility losses can be an appreciable part of the total power, as indicated by figure 2, it is important that the designer be able to predict the tip Mach number and tip angle of attack at which compressibility losses occur.

A comparison of the rotor-blade drag-divergence tip Mach number and angle of attack with unpublished data on the NACA 64_2-015 two-dimensional airfoil section is shown in figure 7. Data on the NACA 64_2-015 airfoil section are used in this comparison since it is the only airfoil similar to the actual rotor blade (NACA 63_2-015) on which data are available. The NACA 64_2-015 airfoil would be expected to have about the same drag-divergence Mach number as the NACA 63_2-015 airfoil.

Data are presented (fig. 7) for the rotor blade in both the smooth condition and with leading-edge roughness added. The results show that at the low-tip-pitch angles the smooth rotor-blade drag-divergence Mach numbers are slightly higher than those indicated by the two-dimensional data. This increase in tip Mach number for drag divergence has been shown in other rotor and propeller tests and is sometimes called a "tip relief effect." It is attributed to the three-dimensional air flow over and around the blade tip which reduces the air-flow velocity over the blade tip section and thus allows a slight increase in tip speed before drag divergence occurs as compared with the two-dimensional flow over the airfoil. As the angle of attack is increased past about 8°, the experimental rotor-blade drag-divergence Mach number drops below that indicated by the two-dimensional data.

A possible explanation of the reduced experimental rotor-blade tip angle of attack lies with the theory from which the tip angle of attack

is calculated. The calculation does not take into account the redistri-
bution of the induced flow (when loss of lift occurs) and thus may under-
estimate the rotor-blade angle of attack. Another factor is introduced
because of the blade twist which caused the calculated maximum blade
angle of attack to occur inboard at about 50 percent of the blade radius.
Thus, the tip angle of attack is somewhat lower than that section of the
blade causing the drag rise.

The flagged symbols (fig. 7) indicate the Mach number for drag diver-
gence of the rotor with leading-edge roughness added and show the reduc-
tion in tip angle of attack at which compressibility drag losses occur
for this condition.

In general, the comparison of the rotor-blade drag-divergence Mach
number with that obtained from two-dimensional airfoil tests provides
the designer with a basis on which to predict the onset of compressi-
bility losses.

Comparison of Rotor Blades Having NACA 632-015 Airfoil Sections

With Those Having NACA 23015 Airfoil Sections

The high-tip-speed performance of the present rotor is compared
with that obtained for a rotor having NACA 23015 airfoil sections. Such
a comparison would be expected to demonstrate the superior performance
at high rotor tip speeds that may be obtained with rotors having air-
foils with more favorable pressure distributions at moderately high sub-
sonic Mach numbers. It is therefore pertinent to examine the airfoil-
section characteristics of each rotor to determine the general magnitude
of the high-tip-speed rotor performance differences that might be
expected.

Two-dimensional airfoil drag divergence.- In figure 8 the two-
dimensional airfoil section lift coefficient is plotted as a function
of Mach number for drag divergence for the two airfoils, the NACA 23015
(ref. 9) and the NACA 64_2-015 (unpublished NACA data used in the absence
of NACA 63_2-015 airfoil-section data). The results show that for Mach
numbers between 0.52 and 0.70 the section lift coefficients for drag
divergence of the NACA 64_2-015 airfoil are substantially higher than
those shown for the NACA 23015 airfoil. For example, at a tip Mach num-
ber of 0.60, the NACA 64_2-015 airfoil can operate at about 0.3 section
lift coefficient higher before drag divergence occurred than the NACA
23015 airfoil can. This result represents an increase in the lift coeffi-
cient of a little over 50 percent. At a constant c_l of about 0.6, the
Mach number for drag divergence for the NACA 63_2-015 airfoil is about

15 percent greater than that for the NACA 23015 airfoil. At the very low section lift coefficients (0 to 0.21), the two airfoils have similar Mach numbers for drag divergence. Above $c_l = 1.0$, the NACA 23015 airfoil appears to be superior to the NACA 64_2-015 airfoil, but the data range is insufficient to establish the trend clearly.

Rotor comparison.- The rotor blades having NACA 23015 airfoil sections, used in the previous tests of reference 1, had a ratio of tip chord to root chord of 0.54 and 8° linear washout. The rotor blades having NACA 63_2-015 airfoil sections, used in present tests, had a rectangular plan form and 6.5° of linear washout. Before these rotors can be compared, it is necessary to examine first the effects of twist and taper on the rotor performance.

The effect of blade twist is to reduce the tip angle of attack for a given rotor thrust and rotational speed. The effect of taper (tip chord less than root chord) is to increase the tip angle of attack for a given thrust and rotational speed. Calculations indicate that this effect is not too powerful in that, for rotors of the same solidity and at a blade mean lift coefficient of about 0.3, a ratio of tip chord to root chord of 0.5 increases the tip angle of attack by only about 0.3° over that for the blade of rectangular plan form. The change in tip angle of attack for the blades with -8° of twist and those with -6.5° of twist is also about 0.3°. Consequently, at a given mean lift coefficient, the rotor blades having NACA 23015 airfoil sections, a taper ratio of 0.54, and -8° of twist will have about the same tip section angle of attack as the rotor blades having NACA 63_2-015 airfoil sections, rectangular plan form, and only -6.5° of twist.

In any comparison of performance of rotor blades, however, the rotor-blade surface condition and contour accuracy will have an important bearing on the rotor characteristics. The leading-edge radius of the rotor having NACA 23015 airfoil sections was about 10 percent larger than that of the true airfoil and its oversize may have resulted in a decreased tip Mach number for drag divergence for that rotor. The leading edge of the rotor having the NACA 63_2-015 airfoil section, on the other hand, was very close to that of the true airfoil. Figure 9 shows a comparison of the profile-torque compressibility losses between the rotor having NACA 23015 airfoils and the one having an NACA 63_2-015 airfoil as curves of profile torque ratios $\dfrac{C_{Q,o(\text{measured})}}{C_{Q,o(\text{calculated})}}$ plotted as a function of rotor-blade mean lift coefficient $\overline{c_l}$. The results show that at a tip Mach number of 0.69 the rotor having NACA 63_2-015 airfoil sections can operate at about a 60 percent higher rotor-blade mean lift coefficient without compressibility losses than can either of the rotors having

NACA 23015 airfoil sections. Thus, the increase in section lift coefficient for drag divergence of the NACA 63_2-015 airfoil as compared with the NACA 23015 airfoil that was shown in figure 8 is substantiated by the measured rotor performance.

The rate of growth of the compressibility losses of the NACA 63_2-015 rotor blades with mean lift coefficient following drag divergence is much less than the rate of growth for the NACA 23015 rotor. At a blade mean lift coefficient 0.30 beyond the onset of compressibility losses, the profile-drag torque losses for the NACA 63_2-015 rotor are about twice that calculated without compressibility effects. For the same condition, the NACA 23015 rotor blade has compressibility losses nearly three times that calculated. Most of this improvement shown by the NACA 63_2-015 rotor blade is believed to be due to the higher airfoil lift coefficient obtained before drag divergence.

Synthesized Characteristics of the NACA 63_2-015 Airfoil

Section for Rotor Performance Calculations

Inasmuch as there were no experimental data available on the high-speed characteristics of the two-dimensional NACA 63_2-015 airfoil section, rotor-blade airfoil-section drag and lift curves as a function of Mach number were synthesized from the experimental rotor performance. The object of such work was to present airfoil data that could be used in predicting the high-tip-speed performance of rotors having similar airfoils. The drag and lift curves herein are based, to a large extent, on unpublished wind-tunnel data on the high-speed characteristics for the two-dimensional NACA 64_2-015 airfoil section. It is believed, however, that the general shape of the section-drag-coefficient curves as a function of Mach number and the drag-divergence Mach numbers are correct but that the section drag coefficients are somewhat high.

In figure 10 the synthesized drag coefficients for the rotor-blade NACA 63_2-015 airfoil section are plotted as a function of Mach number for blade angles of attack from $0°$ to $14°$ and were obtained by subtracting an increment determined by trial and error from the unpublished drag data on the NACA 64_2-015 airfoil section. The resulting curves retain the general shape of the variation of drag with Mach number as that for the unpublished data. The procedure was repeated until the corrected data would accurately predict the relationship to C_T or C_Q over the tip Mach number range of 0.31 to 0.71 covered in the investigation. No attempt was made to correlate C_T or C_Q with the measured blade pitch angle θ.

The synthesized lift coefficient for the rotor-blade NACA 63_2-015 airfoil section is plotted in figure 11 as a function of Mach number for angles of attack from 0° to 14°. The rotor-blade section-lift-coefficient curves were identical to the unpublished lift-coefficient data on the NACA 64_2-015 airfoil section except that the maximum lift-coefficient values were increased to predict accurately the actual experimental rotor performance. Drag and lift curves are presented for Mach numbers up to 0.75 but beyond a Mach number of 0.71 the curves are dashed to indicate their provisional nature.

Generally, the use of the wind-tunnel data on the two-dimensional airfoil section to calculate the increase in rotor power due to compressibility effects results in overestimating the power requirements. This effect is often referred to as a "tip relief effect" wherein the rotor or propeller blade does not experience the same drag, as indicated by two-dimensional data, because of the relieving effect of the air flowing over and around the blade tips. In figures 10 and 11 the "tip relief effect" is already included in the data since the curves were based on the experimental rotor performance. When the rotor performance is calculated by using the data shown in figures 10 and 11, the usual low-speed assumptions, that the outer 3 percent of the blade radius produces no lift but has profile drag, still apply.

CONCLUSIONS

As a result of the high-tip-speed tests, the effect of compressibility on the hovering performance and blade pitching-moment characteristics of a rotor blade having NACA 63_2-015 airfoil sections has been determined experimentally over a tip Mach number range from 0.31 to 0.71. The performance of the test rotor has been compared with that obtained previously with rotor blades having NACA 23015 airfoil sections.

The most significant conclusion is that the differences in Mach number for drag divergence between airfoils shown by two-dimensional data are realized in actual rotor tests. This result then shows that it should be possible to calculate the onset of compressibility drag rise of other rotors based on their two-dimensional section data.

Another important conclusion is that, even though the rotor of the present test had a 15-percent-thick airfoil section, it could operate at a tip Mach number of 0.7 and mean blade lift coefficients of up to about 0.6 before encountering any appreciable compressibility losses. At a tip Mach number of 0.69 the rotor having NACA 63_2-015 airfoil sections, with a thickness distribution developed for more favorable high-tip-speed performance, could reach a 60 percent higher rotor-blade mean

lift coefficient without any compressibility losses as compared with the rotor having NACA 23015 airfoil sections. Some small part of this improvement in performance may be attributable to the more accurate construction of the NACA 63_2-015 rotor blades.

The data also show that the reversal in slope of the blade pitching-moment curve is delayed beyond the onset of compressibility losses.

Synthesized drag and lift characteristic curves for the rotor-blade airfoil section are presented for predicting the high-tip-speed performance of rotors having similar airfoils.

Langley Aeronautical Laboratory,
      National Advisory Committee for Aeronautics,
            Langley Field, Va., August 2, 1956.

REFERENCES

1. Carpenter, Paul J.: Effects of Compressibility on the Performance of Two Full-Scale Helicopter Rotors. NACA Rep. 1078, 1952. (Supersedes NACA TN 2277.)

2. Carpenter, Paul J.: Effect of Wind Velocity on Performance of Helicopter Rotors As Investigated With the Langley Helicopter Apparatus. NACA TN 1698, 1948.

3. Abbott, Ira H., von Doenhoff, Albert E., and Stivers, Louis S., Jr.: Summary of Airfoil Data. NACA Rep. 824, 1945. (Supersedes NACA WR L-560.)

4. Gessow, Alfred: Effect of Rotor-Blade Twist and Plan-Form Taper on Helicopter Hovering Performance. NACA TN 1542, 1948.

5. Gessow, Alfred, and Myers, Garry C., Jr.: Flight Tests of a Helicopter in Autorotation, Including a Comparison With Theory. NACA TN 1267, 1947.

6. Gustafson, F. B., and Gessow, Alfred: Effect of Rotor-Tip Speed on Helicopter Hovering Performance and Maximum Forward Speed. NACA WR L-97, 1946. (Formerly NACA ARR L6A16.)

7. Bailey, F. J., Jr.: A Simplified Theoretical Method of Determining the Characteristics of a Lifting Rotor in Forward Flight. NACA Rep. 716, 1941.

8. Loftin, Laurence K., Jr., and Smith, Hamilton A.: Aerodynamic Characteristics of 15 NACA Airfoil Sections at Seven Reynolds Numbers From 0.7×10^6 to 9.0×10^6. NACA TN 1945, 1949.

9. Graham, Donald J., Nitzberg, Gerald E., and Olson, Robert N.: A Systematic Investigation of Pressure Distributions at High Speeds Over Five Representative NACA Low-Drag and Conventional Airfoil Sections. NACA Rep. 832, 1945.
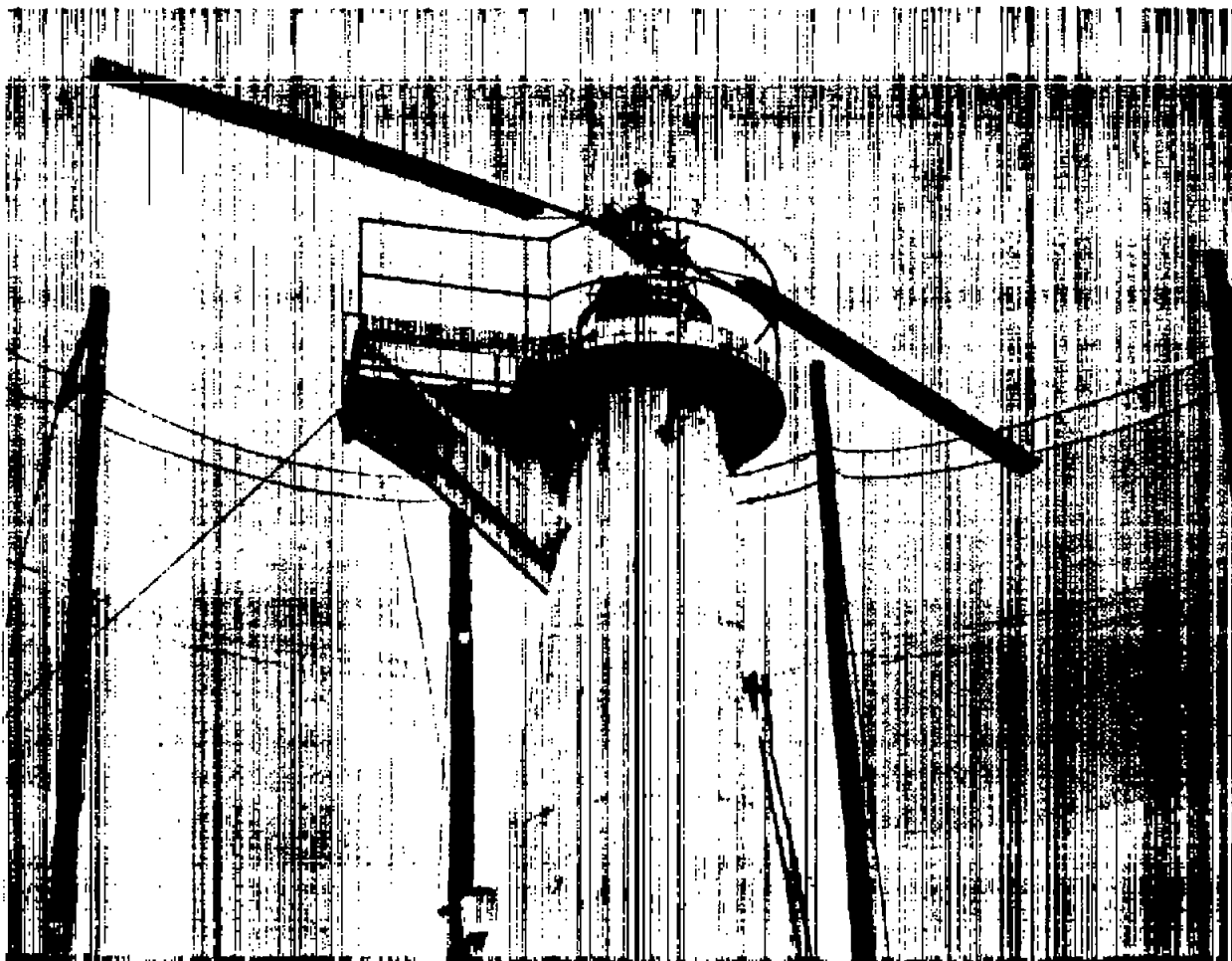
L-89655

Figure 1.- Rotor blades having NACA 63_2-015 airfoil sections mounted on the Langley helicopter test tower.
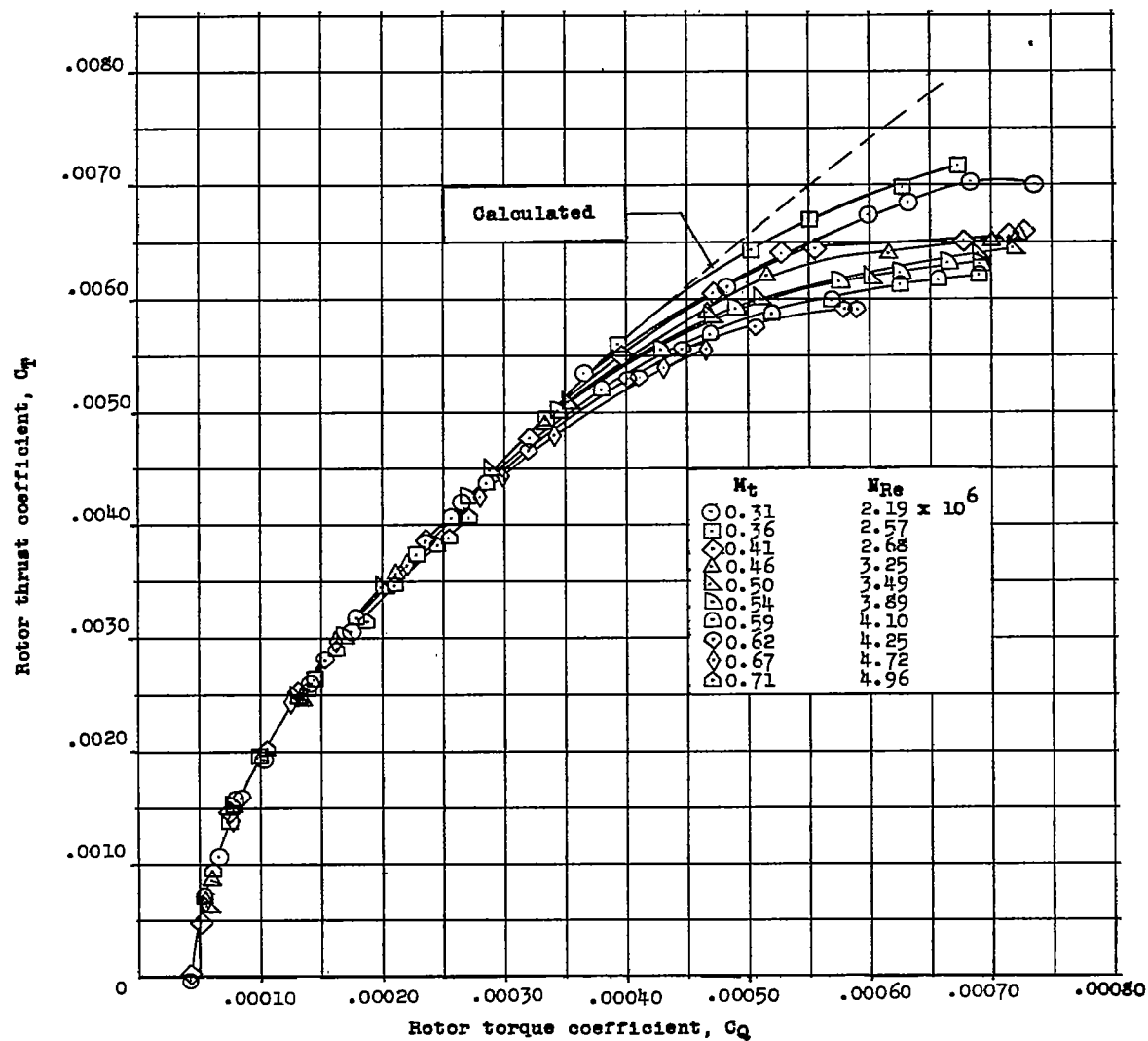
Figure 2.- Hovering performance of rotor blades having NACA 63_2-015 airfoil sections. $\sigma = 0.0374$. Calculated curve based on $c_{d,o} = 0.0087 - 0.0216\alpha_r + 0.400\alpha_r^2$ and $c_l = a\alpha_r$.
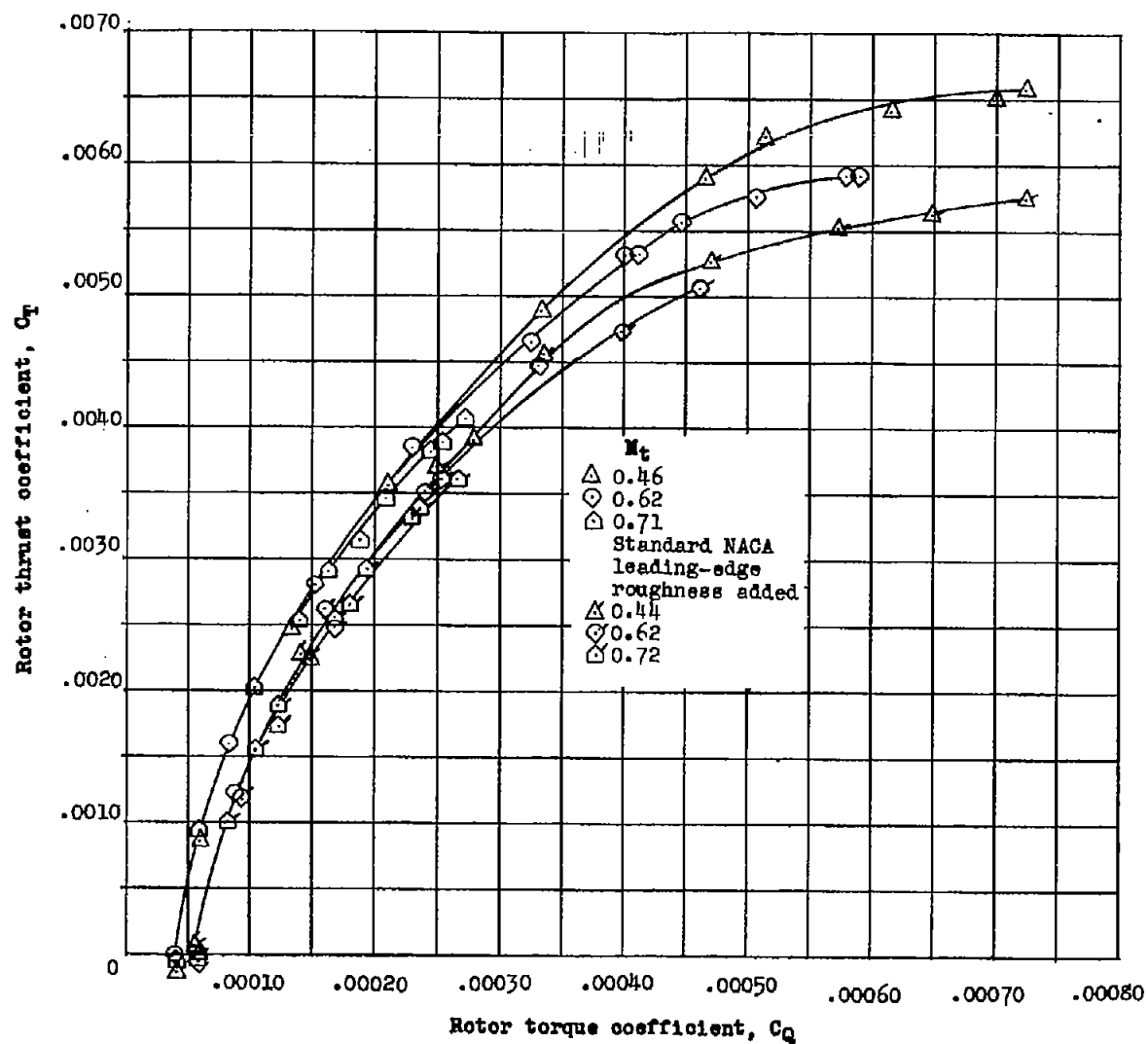
.0070

.0060

.0050

.0040

Rotor thrust coefficient, C_T

.0030

.0020

.0010

0

M_t
△ 0.46
◇ 0.62
⬠ 0.71
Standard NACA
leading-edge
roughness added
△ 0.44
◇ 0.62
⬠ 0.72

.00010   .00020   .00030   .00040   .00050   .00060   .00070   .00080

Rotor torque coefficient, C_Q

Figure 3.- Effect of blade leading-edge roughness on rotor hovering
performance.
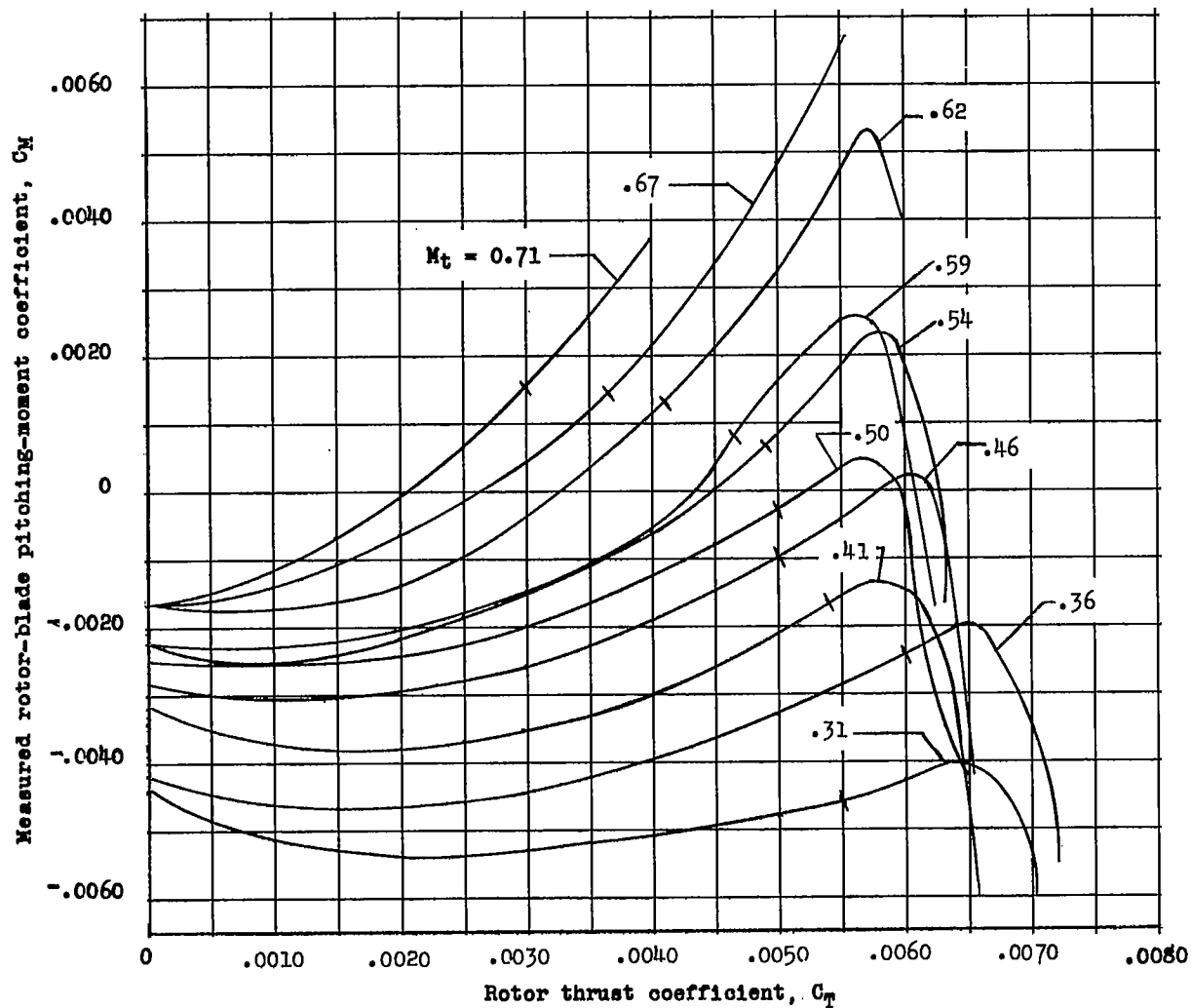
Figure 4.- Pitching moments of rotor blades having NACA 63_2-015 airfoil
sections (smooth). Ticks indicate the onset of compressibility drag
rise.
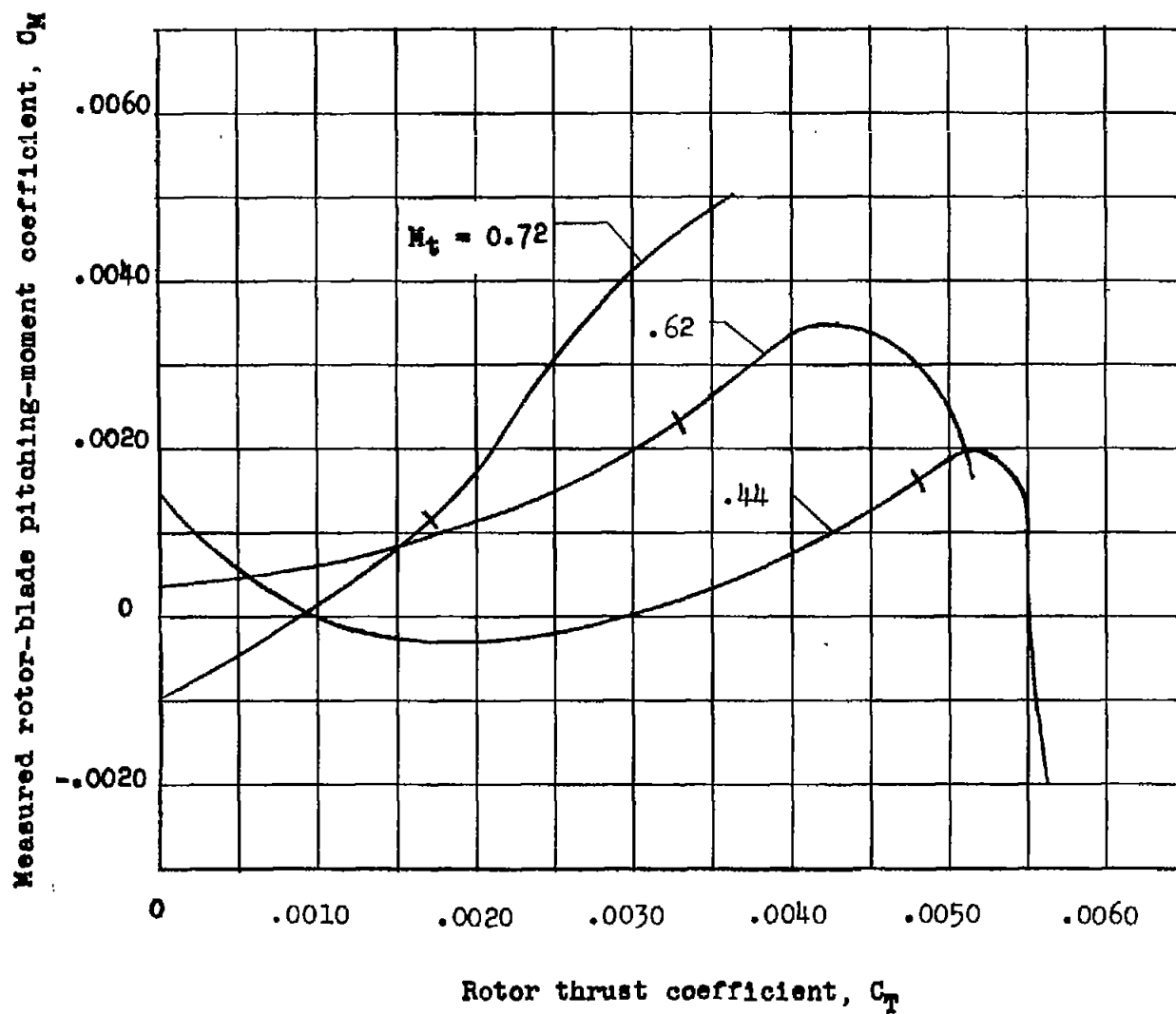
Figure 5.- Effect of blade leading-edge roughness on rotor blade pitching moment. Ticks indicate onset of compressibility drag rise.
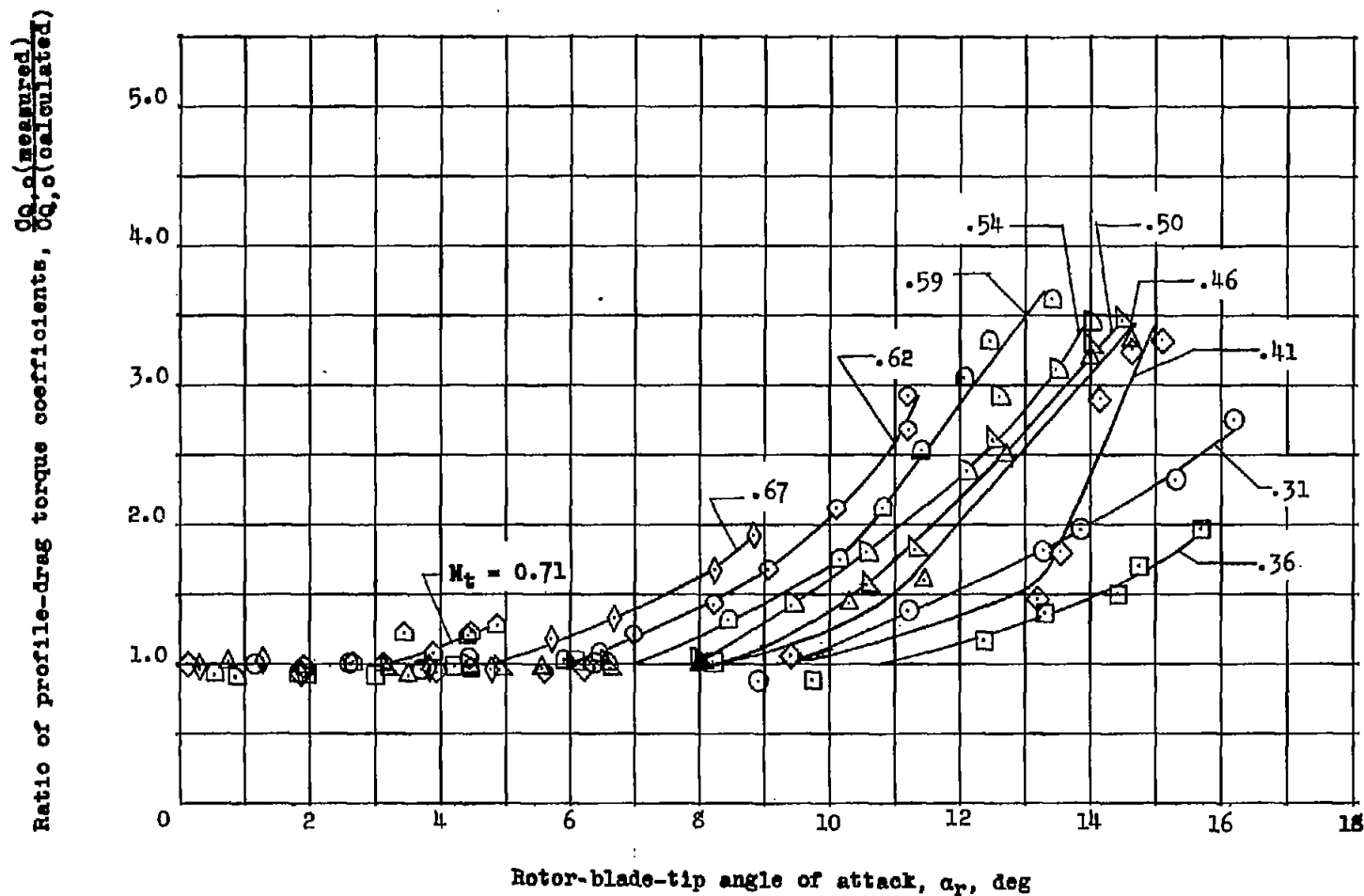
Figure 6.- Effect of tip angle of attack and Mach number on profile-drag torque.
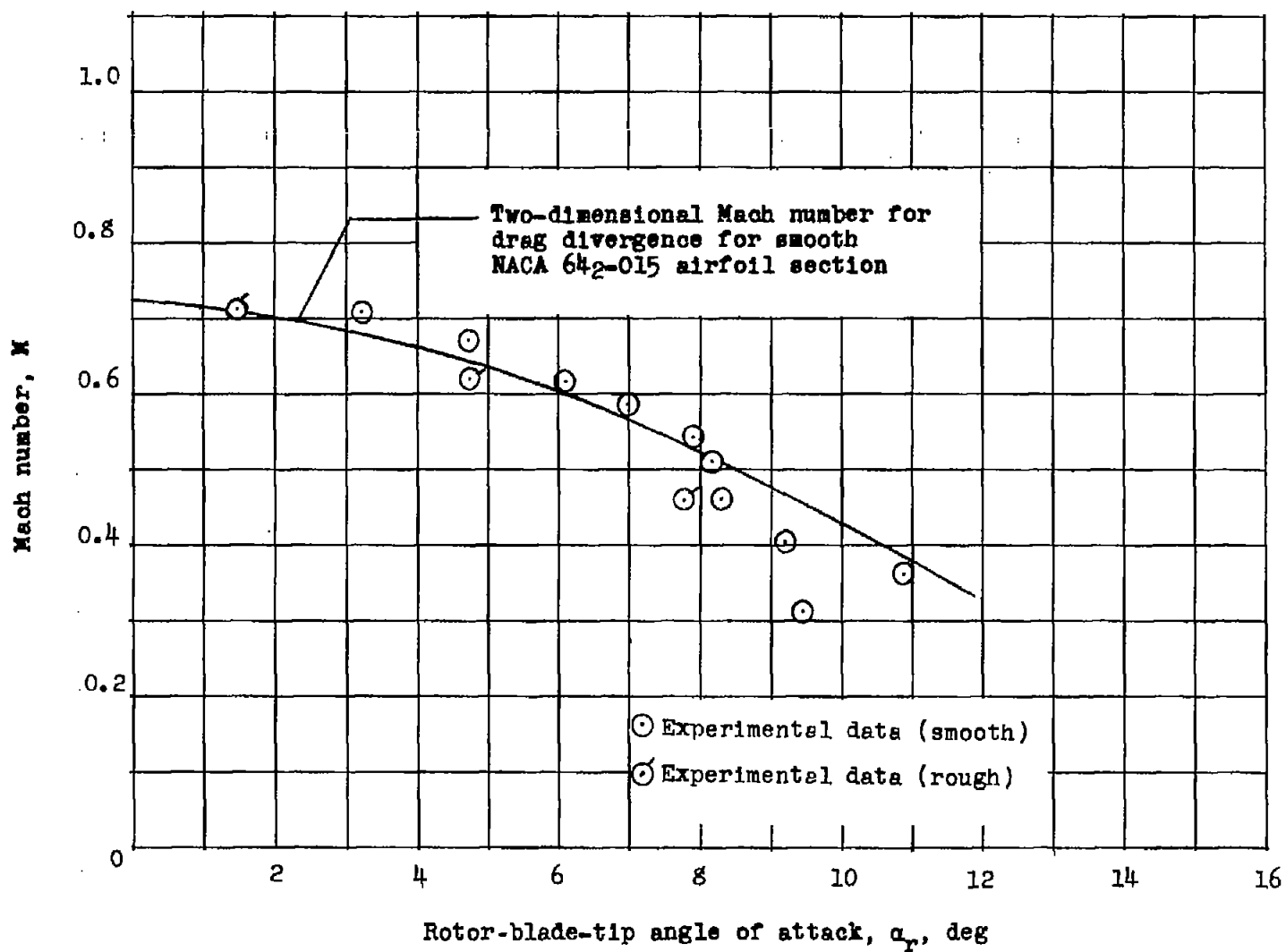
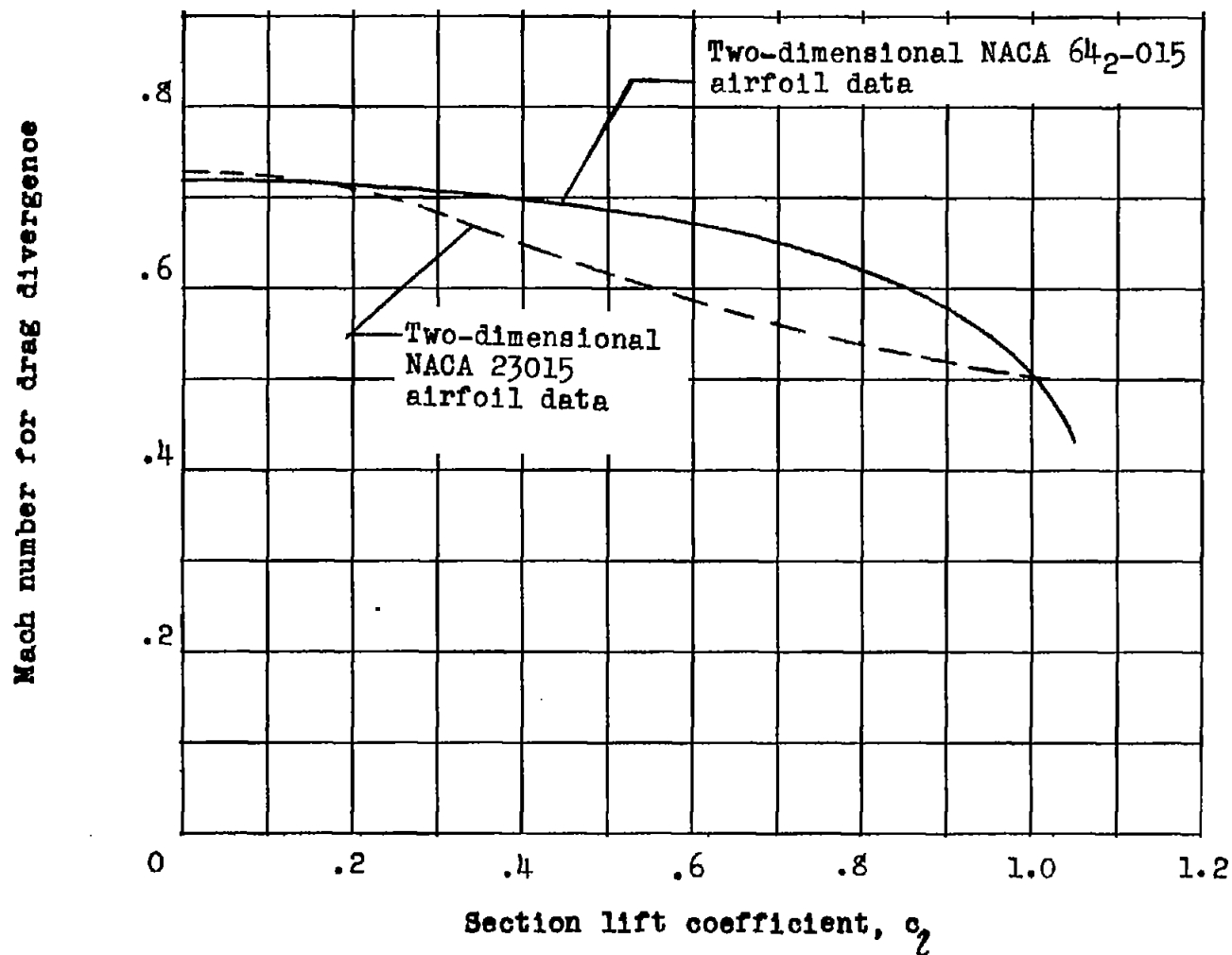Figure 7.- Comparison of rotor experimental results with Mach number for two-dimensional drag divergence for various angles of attack.

Figure 8.- Variation of Mach number for drag divergence with lift coefficient for NACA 64_2-015 and NACA 23015 airfoil sections.
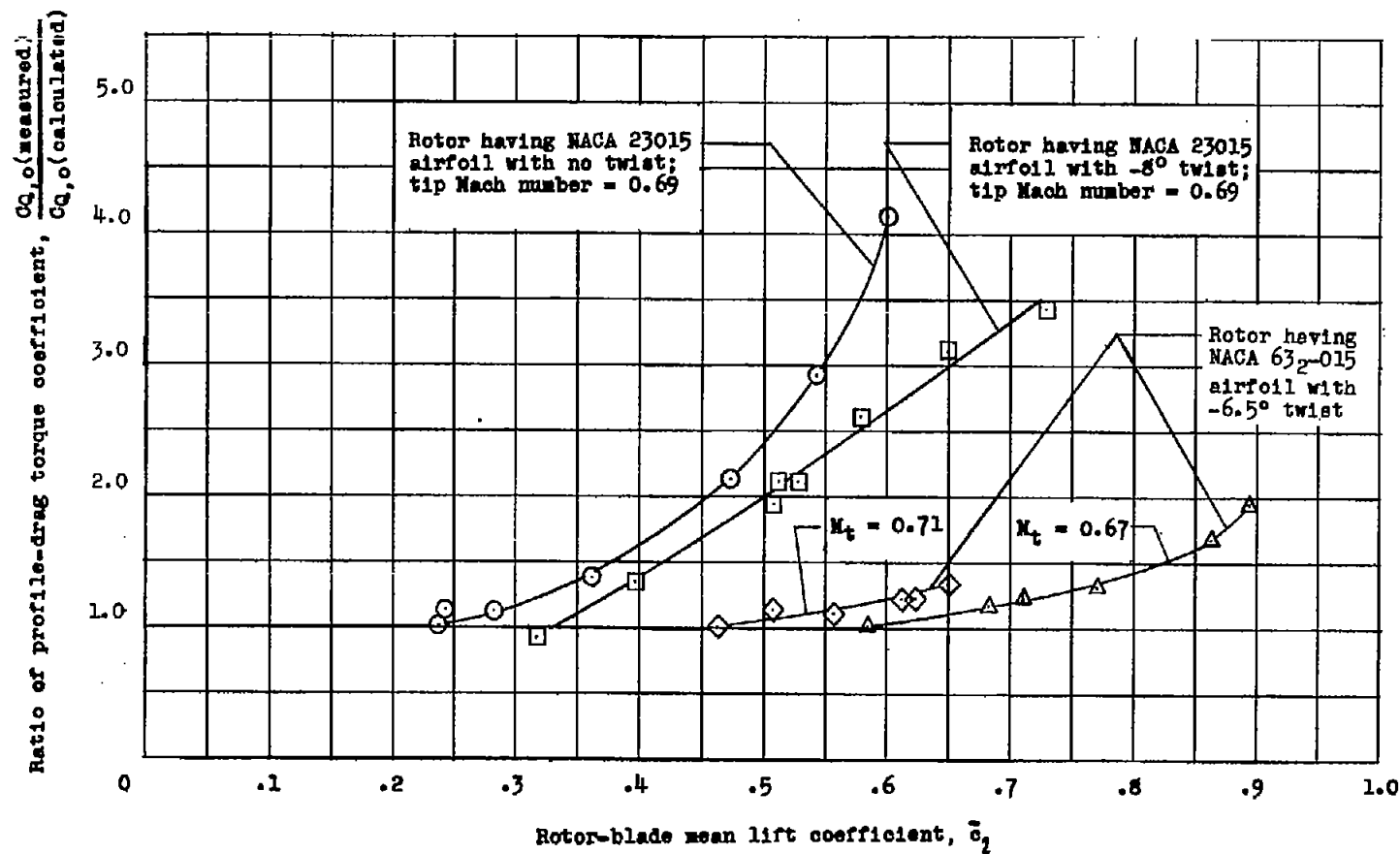
Figure 9.- Comparison of profile-drag torque increase for three rotors
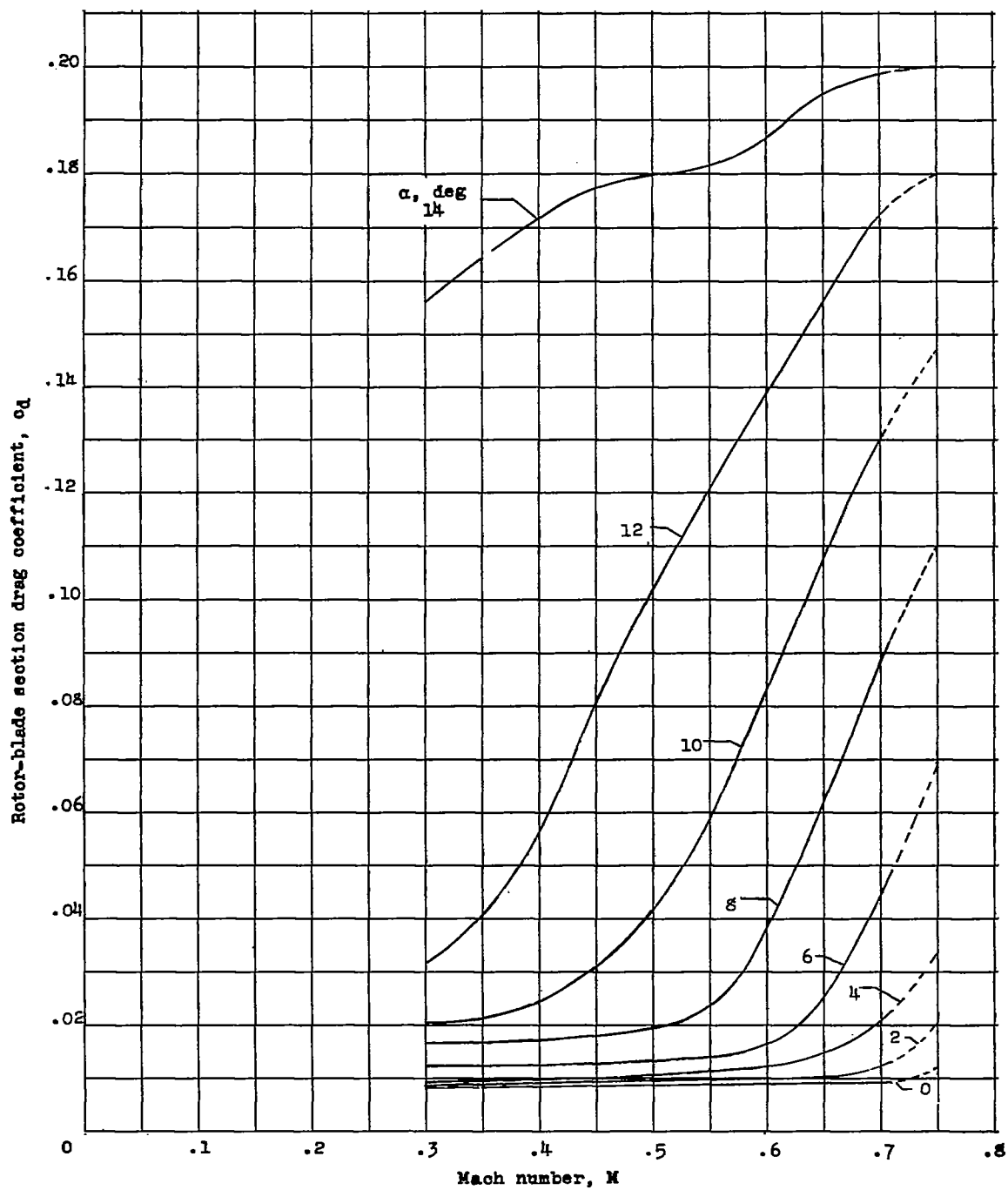having 15-percent-thick airfoils.

Figure 10.- Synthesized rotor-blade section drag coefficient plotted
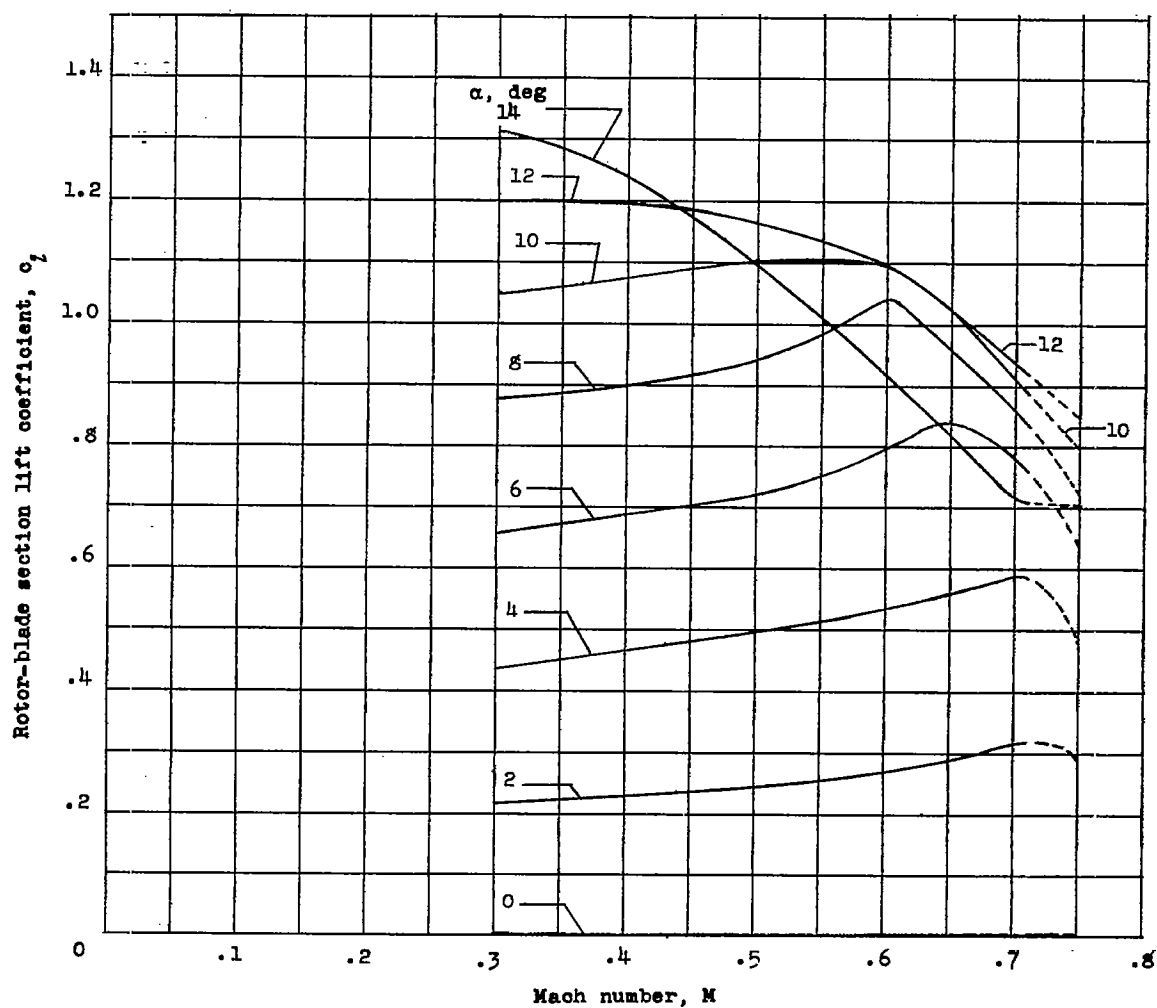against Mach number for NACA 63$_2$-015 airfoil.

Figure 11.- Synthesized rotor-blade section lift coefficient plotted against Mach number for NACA 63_2-015 airfoil.